ELSEVIER

Polymer 41 (2000) 891–898

polymer

Crystallization kinetics of maleic anhydride grafted polypropylene ionomers

J. Yu, J. He*

State Key Laboratory of Engineering Plastics, Institute of Chemistry, The Chinese Academy of Sciences, Beijing 100080, People's Republic of China

Received 8 December 1998; received in revised form 16 March 1999; accepted 16 March 1999

Abstract

Polypropylene (PP) was lightly maleated by solid-state graft polymerization and further neutralized to prepare semicrystalline ionomers, H^+-, Na^+-, Ca^{2+}- and Mn^{2+}-form maleated PP (mPP). The crystallization kinetics of pure PP and these ionomers have been investigated under isothermal and non-isothermal conditions. Under both conditions, the introduction of pendant groups along the PP chains increases the crystallization rate and does not influence the crystallization mode. The energy required for folding macromolecules to form nuclei becomes smaller in case of ionomers. The facility of nucleation in ionomers by the ionic interactions may result in high crystallization rate, while the decrease of chain diffusion in mPP ionomers has a reverse effect at the same time.

Keywords: Isothermal and non-isothermal crystallization kinetics; Maleic anhydride grafted polypropylene; Ionomers

1. Introduction

It is well known that polypropylene (PP), as a consequence of its non-polarity and crystallizability, exhibits very poor compatibility and adhesion towards other materials such as polymers, metals and inorganic fillers. In recent years, grafting of polar monomers, such as maleic anhydride (MAH), on polyolefins has attracted great attention. The polar groups introduced may increase the compatibility and the special interactions and lead to the formation of adhesion with the materials mentioned above.

The graft polymerization of polar monomers onto polyolefins in the presence of a radical initiator is probably the simplest, most widely used method, especially with peroxide initiators. There are many works focusing on the grafting on PP, in both solution-state [1,2] and melt-state [3–5]. Recently, a novel method, solid-state graft polymerization, has been developed by Lee et al. [6–8] to prepare maleic anhydride grafted PP (referred as maleated PP, mPP, hereafter). In this process, the reaction temperature was well below the melting point of PP, alleviating the side reactions of chain scission appeared in melt-state graft polymerization; and a small quantity of organic solvent was used as the interfacial agent, avoiding the recovery of solvent needed in the solution-state graft polymerization. The reaction was performed using a powder-form polymer that remained powder-like during the entire reaction. The validity of this method has been proved by FTIR and the process of graft has been confirmed by solid-state NMR spectroscopy [9]. Interfacial agents such as xylene and decalin were used to swell the polymer and also to provide a medium for the delivery of monomer and free radical initiator to the reactor. They enhanced the graft level. The size of the polymer powder also influenced the graft level, the smaller the size, the higher the graft level because of the higher specific surface area. It was thought that the solid-state graft polymerization took place only on the plane of crystal, the crystal defect and the amorphous region of polymer [10].

Up to now, only a few studies have been reported on the crystallization behaviors of mPP and its ionomers. These studies report the lattice structure of maleated polyolefins [11,12]. As for the crystallization behaviors of the semicrystalline ionomers, ethylene–methacrylic acid (E–MAA) based systems are the ionomers of primary investigation [13–16]. Semicrystalline ionomers are expected to have a crystalline phase with a certain lamella thickness dispersed in an amorphous polymer matrix containing an ion-rich phase, which is roughly depicted by the structural model proposed by Longworth and Vaughan [17] for the ethylene ionomer. It is noticed that the polymer chains interpenetrate into both phases. More recently, some authors have also focused their studies on lightly sulfonated syndiotactic

* Corresponding author. Tel.: +86-10-6261-3251; fax: +86-10-6256-9564.

E-mail address: hejs@sklep.icas.ac.cn (J. He)

0032-3861/00/$ - see front matter
PII: S0032-3861(99)00271-2

polystyrene (SsPS) ionomers. Orler et al. [18,19] studied the effect of alkali metal counterion type on the crystallization kinetics of SsPS. They found that between 180 and 215°C, the rate of crystallization was inversely proportional to the ionic radii of the counterions.

In this study, lightly maleated PP was prepared by solid-state graft polymerization, together with various semicrystalline ionomers based on this mPP. Crystallization kinetics of the samples were investigated under isothermal and non-isothermal crystallization conditions. Moreover, the reasons were also discussed about the differences in crystallization behaviors among pure PP and various ionomers.

2. Experimental

2.1. Materials

The isotactic PP (grade PP 2401 from Yanshan Petrochemical Industrial Co., China) was used as received in powder form. The radical initiator, benzoyl peroxide (BPO), was purified by recrystallization with acetone. MAH and other reagents were of reagent grade without further purification.

mPP (or H^+-form mPP hereafter) samples were prepared by solid-state graft polymerization of PP with MAH using BPO as the initiator [7]. To determine the MAH content, 0.7–1.0 g samples of mPP were dissolved in 100 ml of xylene and refluxed with excess ethanolic KOH for 1 h, using thymol blue as an indicator. The hot solution was back titrated immediately to a yellow end point by the addition of isopropanolic HCl.

In this study, the mPP sample with MAH content of 1.5 mol% was neutralized to produce ionomers. mPP was dissolved in xylene and neutralized by adding stoichiometric amount of NaOH, calcium acetate and manganese acetate (all in ethanol), respectively, from a dropping funnel with stirring. And the mixtures were refluxed for 4 h under a nitrogen purge. The ionomers precipitated in acetone were washed with ethanol several times and dried in vacuum at 60°C for 24 h. Complete neutralization was confirmed by the disappearance of peaks in the range of 1700–1900 cm^{-1} and the appearance of peaks ranged from 1480 to 1670 cm^{-1} in the FTIR spectra. The ionomers are referred to as Na^+-form mPP, Ca^{2+}-form mPP and Mn^{2+}-form mPP hereafter, respectively.

2.2. Thermal analysis

The crystallization behaviors were investigated by using a Perkin–Elmer DSC-7 differential scanning calorimeter. Before the data gathering, all samples were heated to 210°C and held in the molten state for 5 min to eliminate the influence of thermal history. All operations were carried out under a nitrogen environment. Samples weights were between 4–7 mg.

In isothermal crystallization experiments, the sample melts were subsequently quenched to the crystallization temperatures, at a rate of 80°C/min. The exotherms were recorded at selected crystallization temperatures: 124, 125, 126, 127 and 128°C, respectively.

Non-isothermal crystallization experiments were carried out by cooling samples from 210°C to ambient temperature using different cooling rates. The exotherms as a function of temperature were recorded with the cooling rates 5, 10, 15 and 20°C/min, respectively.

2.3. Theory of crystallization

The Avrami [20,21] equation has been proposed to analyze the isothermal crystallization of polymers:

$$X_t = 1 - \exp(-Z(T)t^n), \tag{1}$$

where n is the Avrami exponent, $Z(T)$ the Avrami rate constant and X_t the relative crystallinity at time t, defined by

$$X_t = \frac{X_t(t)}{X_t(\infty)} = \frac{\int_0^t (\mathrm{d}H(t)/\mathrm{d}t)\,\mathrm{d}t}{\int_0^\infty (\mathrm{d}H(t)/\mathrm{d}t)\,\mathrm{d}t}, \tag{2}$$

where $(\mathrm{d}H(t)/\mathrm{d}t)$ represents the heat flow. $X_t(t)$ and $X_t(\infty)$ denote the absolute crystallinity at time t and at the termination of the crystallization process, respectively.

Differentiating Eq. (1) twice, and when $\mathrm{d}^2X_t/\mathrm{d}t^2 = 0$, the time at maximum heat flow t_{max} can be

$$t_{max} = [(n-1)/nZ(T)]^{1/n} \tag{3}$$

and let Eq. (1) equal to 0.5, crystallization half-time, $t_{1/2}$, defined as the time to a relative crystallinity of 50%, can be obtained:

$$t_{1/2} = \left(\frac{\ln 2}{Z(T)}\right)^{1/n}. \tag{4}$$

The Avrami equation has been extended by Ozawa [22] from the theory of Evans for isothermal crystallization to develop a simple method to study the non-isothermal experiment. The general form of Ozawa theory is written as follows:

$$X_t = 1 - \exp[-K(T)/\phi^m], \tag{5}$$

where $K(T)$ is the cooling crystallization function, ϕ the cooling rate and m the Ozawa exponent that depends on the dimension of the crystal growth.

In addition, the Avrami equation can also be used to analyze the non-isothermal crystallization data directly [23]. However, the values of n' and $Z(T)'$ are temperature-dependent, they have different physical meaning as in the isothermal crystallization.

Mo et al. [24] have proposed a new kinetic equation of non-isothermal crystallization by combining the Avrami and Ozawa equations:

$$\ln \phi = \ln F(T) - a \ln t, \tag{6}$$

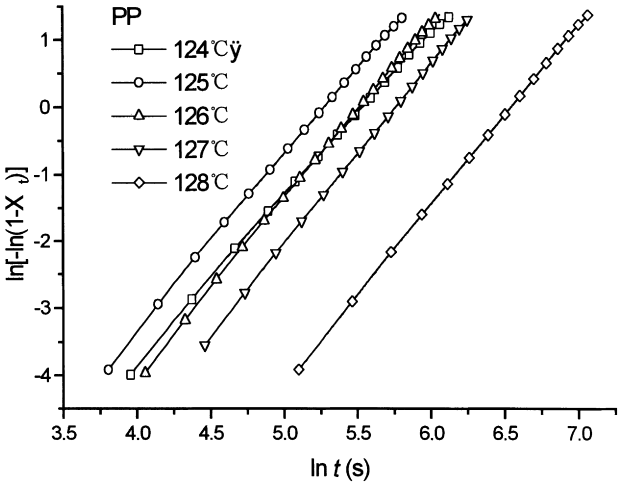

Fig. 1. Avrami plots for isothermal crystallization of pure PP at various temperatures.

where $a = n/m$; the parameter $F(T) = [K(T)/Z(T)]^{1/m}$ refers to the value of the cooling/heating rate, which has to be chosen at unit crystallization time when the measured system amounts to a certain degree of crystallinity. According to Eq. (6), the plot of ln ϕ versus ln t at a given crystallinity will be a straight line. Parameters a and $F(T)$ can be obtained from the slope and the intercept of the line.

It is shown that Eq. (6) is valid even in the non-isothermal crystallization of polymers, where the Ozawa theory cannot adequately describe the kinetics because of its secondary crystallization [24].

3. Results and discussion

3.1. Isothermal crystallization

The typical Avrami plots obtained at various temperatures are illustrated for pure PP in Fig. 1. Other samples, H^+-form mPP and neutralized ionomers based on H^+-form mPP, have the similar Avrami plots. There are good linearities of $\ln[-\ln(1 - X_t)]$ versus $\ln t$ in a wide relative crystallinity range (2–90%). It is clear that the Avrami equation is quite successful for analyzing the experimental data of the isothermal crystallization kinetics. The Avrami exponent n and the rate constant $Z(T)$ can be obtained from the values of the slope and intercept of these straight lines. The values of $Z(T)$, n, $t_{1/2}$ and t_{max} are listed in Table 1. The data shows that the $t_{1/2}$ and t_{max} of all samples except PP increase with increasing crystallization temperature, indicating that their crystallization processes are controlled by the nucleation, while PP has its smallest $t_{1/2}$ and t_{max} at 125°C under experimental conditions. Depending on the mechanism of nucleation and crystal growth, n should be different integer values,

Table 1
The various parameters of samples from the Avrami equation

Sample	T_c (°C)	$Z(T)$ (s^{-n})	n	t_{max}[a] (s)	$t_{1/2}$[b] (s)	t_{max}[c] (s)	$t_{1/2}$[c] (s)
PP	124	1.57×10^{-6}	2.41	204.0	218.8	203.4	218.5
	125	1.27×10^{-6}	2.57	161.9	170.0	156.6	169.4
	126	4.92×10^{-7}	2.63	208.2	217.2	207.0	216.3
	127	1.85×10^{-7}	2.69	268.0	278.0	271.8	278.2
	128	2.44×10^{-8}	2.68	585.3	607.8	577.8	608.8
H^+-form mPP	124	4.70×10^{-6}	2.53	104.6	110.4	95.4	108.4
	125	1.54×10^{-6}	2.62	137.8	143.9	127.8	141.5
	126	7.03×10^{-7}	2.64	177.8	185.3	163.8	182.0
	127	3.41×10^{-7}	2.65	230.7	240.2	212.4	235.3
	128	2.94×10^{-8}	2.71	506.6	524.4	481.5	514.2
Na^+-form mPP	124	3.25×10^{-4}	2.62	17.8	18.6	14.4	18.4
	125	1.42×10^{-4}	2.55	26.5	27.9	23.4	27.7
	126	5.11×10^{-5}	2.65	35.0	36.5	32.4	36.0
	127	3.76×10^{-5}	2.58	42.6	44.7	39.6	44.2
	128	2.99×10^{-5}	2.52	50.9	53.8	46.8	53.1
Ca^{2+}-form mPP	124	3.66×10^{-5}	2.89	29.7	30.4	27.0	30.4
	125	1.85×10^{-5}	2.88	37.8	38.6	36.0	38.5
	126	8.91×10^{-6}	2.89	48.6	49.6	46.8	49.4
	127	2.17×10^{-6}	3.02	65.3	66.1	63.0	65.6
	128	1.08×10^{-6}	3.00	84.6	85.7	81.0	85.0
Mn^{2+}-form mPP	124	3.10×10^{-5}	2.75	37.1	38.3	34.2	37.7
	125	8.84×10^{-6}	2.88	49.3	50.4	45.0	49.4
	126	3.97×10^{-6}	2.91	62.3	63.5	57.6	62.7
	127	1.91×10^{-6}	2.91	79.9	81.5	73.8	80.3
	128	7.51×10^{-7}	2.95	103.2	104.9	97.2	103.6

[a] Calculated from Eq. (3).
[b] Calculated from Eq. (4).
[c] Obtained from experimental data.

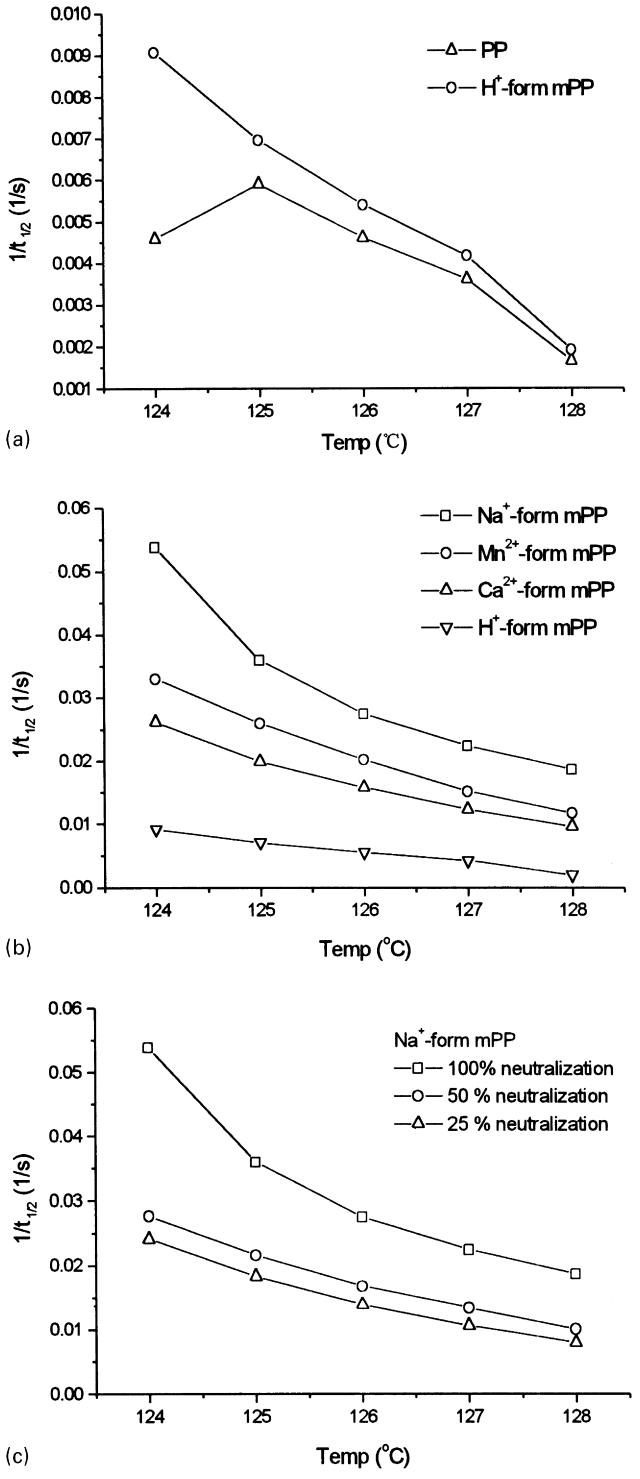

Fig. 2. (a) Plots of $t_{1/2}^{-1}$ versus crystallization temperature of PP and H^+-form mPP. (b) Plots of $t_{1/2}^{-1}$ versus crystallization temperature of various ionomers. (c) Plots of $t_{1/2}^{-1}$ versus crystallization temperature of Na^+-form mPP with different neutralization.

predicted by the theory. But the non-integer values of the Avrami exponent are obtained for all the samples from experimental data, for example in the range of 2.4–2.9 and 2.5–3.0 at crystallization temperatures, 124 and 128°C, respectively. It is caused by some characters of polymers not matching the simplification in the Avrami equation, such as secondary crystallization process, mixed nucleation modes and the change in material density [25]. Moreover, even some experimental factors [26], such as an error introduced in the determination of the zero point of crystallization can lead to non-integer value of n. The variation of n can be neglected within the error range in this study. The graft reaction takes place only on the sites of crystal planes, crystal defects and amorphous regions of PP during solid-state graft polymerization [10], which has little influence on the crystallization mode. Therefore, the crystallization mode of PP is suggested to be unchanged after solid-state graft polymerization and further neutralization.

The values of t_{max} and $t_{1/2}$ obtained from experimental data are also given in Table 1. They are consistent with those calculated from Eqs. (3) and (4), indicating the validity of the Avrami equation in this study.

Fig. 2(a) shows the comparison of the reciprocal of $t_{1/2}$, which characterizes the crystallization rate, against crystallization temperature T_c of PP and H^+-form mPP. Fig. 2(b) shows those of the samples neutralized with different ions. The crystallization rate of ionomers is about one order magnitude greater than that of pure PP, and this is more obvious at lower crystallization temperature. Among ionomers neutralized by different ions, the Na^+-neutralized ionomer has the highest crystallization rate. It is generally accepted that ionic groups in the ionomers associate to form ionic domains, including multiplets and/or clusters because of ionic interaction [27]. Multiplets can exist even at temperatures above the melting point of the semicrystalline matrix. They will act as nuclei during the crystallization process. To better elucidate the influence of ionic interaction on the crystallization, the kinetics has been studied further for the Na^+-form mPP with 50 and 25% neutralization under the same conditions of Fig. 2(a) and (b). The change of $t_{1/2}$ as a function of T_c is shown in Fig. 2(c). For the Na^+-neutralized ionomers, the crystallization rate increases monotonically with increasing neutralization extent. It is because more ionic domains are formed by higher neutralization of samples with a certain graft level. Therefore, the significant increase in nucleation leads to a higher crystallization rate of the ionomers.

According to the Hoffman theory, the growth rate of crystals, G, can be expressed as follows [28]:

$$G = G_0 \exp\left[-\frac{\Delta F}{RT_c}\right]\exp\left[-\frac{k_g T_m^0}{T_c \Delta T}\right], \quad (7)$$

where G_0 is a constant, R the molar gas constant and ΔF the activation energy for the transport process at the interface, related to the molecule construction and temperature. Supercooling $\Delta T = T_m^0 - T_c$, T_m^0 is the equilibrium melt point. The WLF expression for the temperature dependence

Table 2
Various parameters of PP for the Hoffman theory [29]

Parameter	T_m^0 (K)	T_g (K)	ΔH (J/m^3)	b_0 (m)	σ (J/m^2)	σ_e (J/m^2)
Value	481	265	134×10^6	6.56×10^{-10}	8.79×10^{-3}	0.157

of polymer viscosity is used for the determination of ΔF:

$$\Delta F_{WLF} = \frac{C_1 T_c}{C_2 + (T_c - T_g)} \quad (8)$$

where, the ordinary parameters $C_1 = 17.22$ kJ/mol and $C_2 = 51.6$ K. Constant

$$k_g = \frac{4 b_0 \sigma \sigma_e}{k \Delta H} \quad (9)$$

where b_0 is the thickness of the surface layer, defined by the crystalline lattice parameters. σ and σ_e are interfacial free energies per unit area parallel and perpendicular, respectively, to the molecular chain direction. The value of σ can be calculated from an empirical relation given by Hoffman [28]: $\sigma = \beta b_0 \Delta H$, where β is a numerical constant equal to 0.1 for polymers. k is the Boltzmann constant and ΔH is the heat of fusion per unit volume.

The Avrami equation describes the overall crystallization behavior of the whole sample, while the Hoffman theory describes the nucleation and growth of single crystals. Therefore, the overall crystallization rate could be expressed by a generalized equation [29]:

$$\frac{1}{n}\ln Z(T) + \frac{\Delta F}{R T_c} = A_n - \frac{k_g T_m^0}{T_c \Delta T}, \quad (10)$$

where $Z(T)$ and n are the parameters in the Avrami equation. Thus, k_g can be determined graphically from the slope of plot of $(1/n)\ln Z(T) + (\Delta F/RT_c)$ versus $(T_m^0/T_c\Delta T)$, and σ_e can be obtained by substituting k_g into Eq. (9).

All the parameters of PP for Hoffman theory are listed in Table 2. Table 3 shows values of σ_e of the samples in this study. It can be seen that the value of σ_e increases in the following order: neutralized ionomers, maleated polymer and pure PP. Note that σ_e is the interfacial free energy of the side surface of the nuclei, such that the smaller the σ_e, the smaller is the work required in folding the macromolecule. It might be concluded that the introduction of polar groups in the PP chain and counterions in the mPP chain dramatically increases the nucleation rate and hence the overall crystallization rate, which is consistent with the trend of crystallization rate characterized by the reciprocal of $t_{1/2}$.

The counterion can affect the ability of the mPP ionomers to crystallize in two opposite directions. On the one hand, as ion pairs pack into multiplets, a physical cross-linked network is formed by the dipole–dipole interactions between ion pairs. Consequently, the mobility of the polymer chain diminishes. The stronger the interaction is, the slower the crystallization rate [18]. On the other hand, existing ion pairs and multiplets can act as heterogeneous nuclei in the nucleation of crystallization. The increase of the nucleus density has a positive effect on crystallization. Moreover, the energy to form a nucleus of critical size, which is disclosed by σ_e shown in Table 3, decreases for various forms of mPP, compared with pure PP.

3.2. Non-isothermal crystallization

From a technological point of view, non-isothermal crystallization conditions approach more closely the industrial conditions of polymer processing, so that the study of crystallization of polymers under non-isothermal conditions is of great practical importance. At the same time, because of more errors of the crystallization rates of the samples at too high or too low crystallization temperatures, the isothermal measurement is often restricted to narrow temperature windows. Consequently, non-isothermal crystallization is often conducted to complement the isothermal data. However, there are only a few methods developed to study the kinetics of non-isothermal crystallization of polymers. Lopez et al. [30] gave a very useful discussion about these methods, but none of these methods is convenient enough for analyzing the non-isothermal data. Mo et al. [24] developed a new simple method by combining the Avrami equation and the Ozawa method, and demonstrated its validity for poly(aryl ether ether ketone ketone).

Some temperatures to describe crystallization exotherms are defined below and illustrated in Fig. 3:

1. The peak temperature of the crystallization exotherm, T_{max}, is the temperature where the value of the heat flow is maximum.
2. The onset temperature, T_{onset}, is the temperature at the crossing point of the tangents of the baseline and the high temperature side of the exotherm.

Table 3
The σ_e values of samples from the Hoffman theory

Sample	PP	H^+-form mPP	Na^+-form mPP	Ca^{2+}-form mPP	Mn^{2+}-form mPP
σ_e (J/m^2)	0.254	0.233	0.151	0.177	0.170

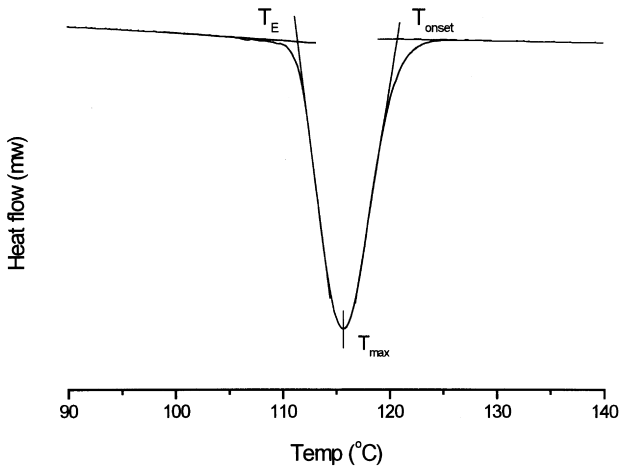

Fig. 3. Schematic representation of the method of determination of various temperatures from DSC crystallization exotherm.

3. The end temperature, T_E, is the temperature at the crossing point of the tangents of the baseline and the low temperature side of the exotherm.

The temperature of the point where the DSC thermogram begins to deviate from the baseline is not adopted in this study, because of the inaccuracy in determining this temperature. Therefore, the relative crystallinity X_c of non-isothermal crystallization is determined by integrating the DSC exotherm peak from T_{onset} to T_E [31], which is a little bit different from the definition of X_t in the isothermal study.

Fig. 4 shows the typical DSC thermograms of non-isothermal crystallization of the Na^+-form mPP at different cooling rates. The parameters of exotherms are listed in Table 4. For all the samples, due to enough time to activate nuclei at low cooling rates, the beginning of the crystallization exotherm appears at smaller supercooling, i.e. at higher temperatures. For a given cooling rate, T_{onset} of the H^+-form mPP is the lowest among the ionomers. As for ($T_{onset} - T_E$), reflecting the width of the crystallization exotherm, the H^+-form mPP samples have the largest values. It is noted that the strength of hydrogen-bond interaction in H^+-form mPP is weaker than the ionic interactions in neutralized ionomers. As a result, the nucleation process of H^+-form mPP is not promoted so much as in neutralized ionomers.

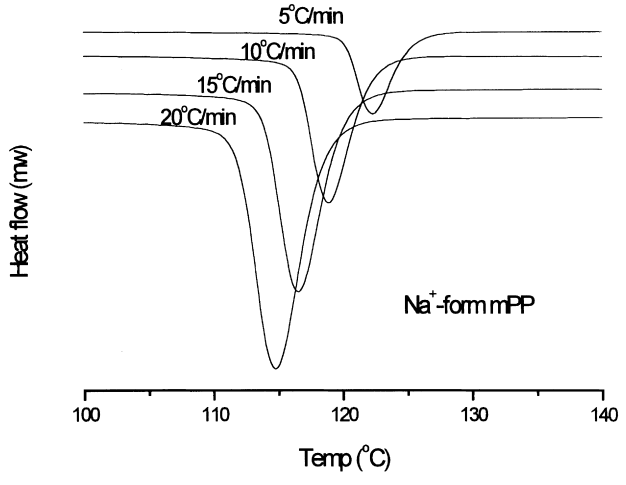

Fig. 4. DSC thermograms of non-isothermal crystallization of Na^+-form mPP at different cooling rates.

In Fig. 5, according to the Avrami equation, the plot of $\ln[-\ln(1 - X_c)]$ versus $\ln t$ is shown. Fitting the Avrami plot with straight line, we can obtain the rate constant Z'_t and the Avrami exponents n' from the slope and intercept, as listed in Table 4. Because the non-isothermal crystallization is a temperature-changing process, the Avrami exponent n' does not have the same physical significance as in the isothermal crystallization. The former would be a summary value of n in the whole temperature range of the exotherm. It is shown from Table 4 that all n' is in a limited range of 2.5–2.6. Therefore, it is consistent with the result of isothermal crystallization, i.e. that the solid-state grafting of PP and neutralization of mPP do not change the crystallization mode of PP. In non-isothermal crystallization, $t'_{1/2}$ decreases with increasing cooling rate because of quickly freezing of chain mobility at high cooling rate.

$F(T)$ and a can be determined from the slope and intercept of double logarithm plot of cooling rate versus crystallization time at different relative crystallinities X_c of 0.2, 0.4, 0.5, 0.6 and 0.8, respectively, according to Eq. (6). Fig. 6 presents the result of Na^+-form mPP. The values of $F(T)$ and a for all the samples are listed in Table 5. At a certain relative crystallinity, a high value of $F(T)$ means a high cooling rate needed to reach this X_c in a unit time, which reflects the difficulty of its crystallization process. Table 5 shows that the value of $F(T)$ increases with increasing relative crystallinity. PP and H^+-form mPP have the largest and the lowest values of $F(T)$, respectively, among all the samples at these selective X_c's, implying the slowest and the fastest crystallization rate of PP and H^+-form mPP. This conclusion is different from the results obtained from isothermal analysis. It might be due to the lower peak temperature T_{max} of H^+-form mPP than other samples, shown in Table 4. Lower crystallization temperature, hence the higher supercooling, is in favor of crystallization in the study. Other ionomers have higher T_{max} values than PP and H^+-form mPP, but their $F(T)$'s are still lower than those of PP and close to those of H^+-form mPP, showing a rather rapid process of the non-isothermal crystallization and higher rates of crystallization in these ionomers. It means the introduction of ion groups contributes to the acceleration of crystallization, which has been shown in isothermal analysis.

4. Conclusions

The crystallization kinetics of pure PP, H^+-form mPP and other forms of ionomers have been investigated under isothermal and non-isothermal conditions. Under both

Table 4
The various parameters of samples from DSC non-isothermal crystallization exothermic peaks

Samples	ϕ (°C/min)	T_{max} (°C)	T_{onset} (°C)	$T_{onset} - T_E$ (°C)	Z'_t (s^{-n})	n'	$t'_{1/2}$ (s)
PP	5	115.7	120.9	10.4	2.06×10^{-5}	2.56	58.7
	10	111.7	117.7	12.0	8.83×10^{-5}	2.55	33.7
	15	108.6	115.5	13.8	1.85×10^{-4}	2.56	24.9
	20	106.0	113.5	15.0	2.83×10^{-4}	2.57	20.8
H^+-form mPP	5	114.8	119.4	9.2	3.80×10^{-5}	2.55	46.9
	10	112.0	115.8	7.6	3.71×10^{-4}	2.50	20.3
	15	110.2	114.0	7.6	7.71×10^{-4}	2.56	14.3
	20	108.0	112.8	9.6	1.42×10^{-3}	2.52	11.7
Na^+-form mPP	5	122.3	125.6	6.6	6.94×10^{-5}	2.54	37.5
	10	118.8	122.5	7.4	3.82×10^{-4}	2.51	19.9
	15	116.5	120.4	7.8	7.30×10^{-4}	2.55	14.7
	20	114.8	118.8	8.0	1.16×10^{-3}	2.58	11.9
Ca^{2+}-form mPP	5	123.5	126.8	6.6	7.69×10^{-5}	2.56	35.1
	10	120.2	123.8	7.2	3.87×10^{-4}	2.52	19.5
	15	117.9	121.8	7.8	5.72×10^{-4}	2.66	14.4
	20	116.1	120.2	8.2	1.19×10^{-3}	2.63	11.3
Mn^{2+}-form mPP	5	118.3	121.9	7.0	5.95×10^{-5}	2.52	41.1
	10	115.0	118.9	7.8	2.60×10^{-4}	2.56	21.8
	15	112.9	117.1	8.4	5.61×10^{-4}	2.60	15.5
	20	111.3	115.7	8.8	1.00×10^{-3}	2.61	12.3

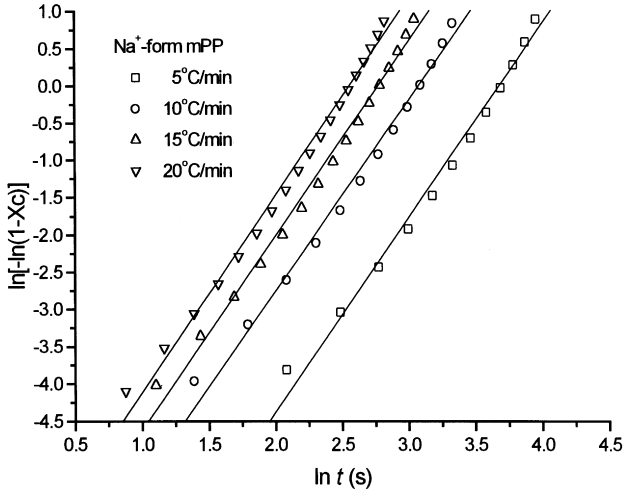

Fig. 5. Plots of $\ln[-\ln(1 - X_c)]$ versus $\ln t$ for Na^+-form mPP.

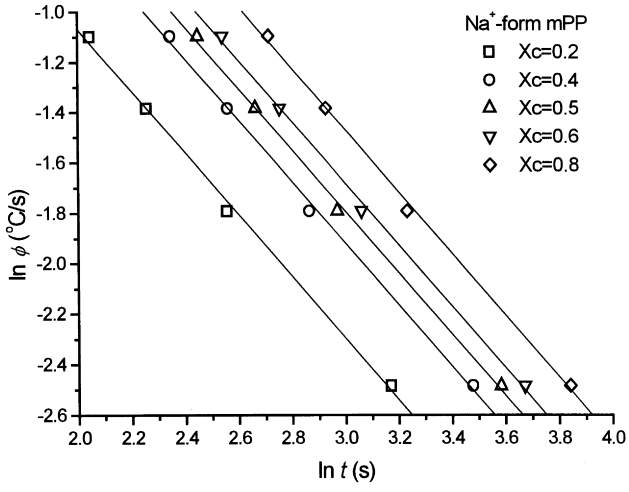

Fig. 6. Plots of $\ln \phi$ versus $\ln t$ for Na^+-form mPP at different relative crystallinities.

Table 5
Non-isothermal kinetics parameters at different relative crystallinities by Eq. (6)

X_c		0.2	0.4	0.5	0.6	0.8
PP	$F(T)$	10.45	16.06	18.72	21.37	26.72
	a	1.32	1.33	1.33	1.33	1.32
H^+-form mPP	$F(T)$	2.28	3.06	3.39	3.73	4.56
	a	0.96	0.96	0.97	0.97	0.98
Na^+-form mPP	$F(T)$	3.98	5.70	6.40	7.24	9.07
	a	1.22	1.22	1.22	1.22	1.23
Ca^{2+}-form mPP	$F(T)$	4.03	5.74	6.51	7.30	9.08
	a	1.23	1.22	1.22	1.22	1.22
Mn^{2+}-form mPP	$F(T)$	3.69	5.19	5.84	6.51	8.02
	a	1.15	1.14	1.14	1.14	1.14

conditions, the introduction of pendant groups along PP chains increases the crystallization rate and does not influence the crystallization mode. The energy required for folding macromolecules to form nuclei becomes smaller in the case of ionomers. The facility of nucleation in ionomers by the ionic interactions may result in high crystallization rates, while the decrease of chain diffusion in mPP ionomers has a reverse effect at the same time.

The counterions introduced affect the crystallization process of the mPP ionomers in two opposite directions, i.e. promoting the nucleation and hindering the chain motion. And the action of these two effects changes with crystallization temperature to a different degree. The ionic interaction decreases and molecular motion increases with

increasing temperature, respectively. As a temperature-changing process, the non-isothermal crystallization is complicated and needs further studies.

References

[1] Minoura Y, Ueda M, Mizunuma S, Oba M. J Appl Polym Sci 1969;13:1625.
[2] Ruggeri G, Aglietto M, Petragnani A, Ciardelli F. Eur Polym J 1983;19:863.
[3] Ho RM, Su AC, Wu CH, Chen SL. Polymer 1993;34:3264.
[4] Gaylord NG, Mishra MK. J Polym Sci Polym Lett Ed 1983;21:23.
[5] Sun YJ, Hu GH, Lambla M. J Appl Polym Sci 1995;57:1043.
[6] Rengarajan R, Vicic M, Lee S. Polymer 1989;30:933.
[7] Rengarajan R, Vicic M, Lee S. J Appl Polym Sci 1990;39:1783.
[8] Lee S, Rengarajan R, Parameswaran VR. J Appl Polym Sci 1990;41:1891.
[9] Rengarajan R, Parameswaran VR, Lee S, Vicic M. Polymer 1990;31:1703.
[10] Shen J, Fan X, Zhao J, Chen S, Huang T. Polym Prepr 1995;36(1):251.
[11] Duvall J, Sellitti C, Myers C, Hiltner A, Baer E. J Appl Polym Sci 1994;52:207.
[12] Weiss RA, Agarwal PK. J Appl Polym Sci 1981;26:449.
[13] Tsujita Y, Shibayama K, Takizawa A, Kinoshita T. J Appl Polym Sci 1987;33:1307.
[14] Prud'homme RE, Stein RS. Macromolecules 1971;4:668.
[15] Quiram DJ, Register RA, Ryan AJ. Macromolecules 1998;31:1432.
[16] Kohzaki M, Tsujita Y, Takizawa A, Kinoshita T. J Appl Polym Sci 1987;33:2393.
[17] Longworth R, Vaughan DJ. Nature 1968;218:85.
[18] Orler EB, Moore RB. Macromolecules 1994;27:4774.
[19] Orler EB, Calhoun BH, Moore RB. Macromolecules 1996;29:5965.
[20] Avrami M. J Chem Phys 1939;7:1103.
[21] Avrami M. J Chem Phys 1940;8:212.
[22] Ozawa T. Polymer 1971;12:150.
[23] Cebe P. Polym Composites 1988;9:271.
[24] Liu TX, Mo ZS, Wang SE, Zhang HE. Polym Eng Sci 1997;37:568.
[25] Srinivas S, Babu JR, Riffle JS, Wilkes GL. Polym Eng Sci 1997;37:497.
[26] Grenier D, Prud'homme RE. J Polym Sci Polym Phys Ed 1980;18:1855.
[27] Eisenberg A. Macromolecules 1970;3:147.
[28] Hoffman JD. SPE Trans 1964;4:315.
[29] Godovsky YuK, Slonimsky GL. J Polym Sci Polym Phys Ed 1974;12:1053.
[30] Lopez LG, Wilkes GL. Polymer 1989;30:882.
[31] Jeziorny A. Polymer 1978;19:1142.